An Initial Investigation for Locating Self-Clearing Faults in Distribution Systems

Charles Kim, *Senior Member, IEEE*, Thomas Bialek, *Member, IEEE*, and Jude Awiylika

***Abstract*—An approach of inverse time-domain transient analysis is devised as a possible method of locating self-clearing, sub-cycle incipient faults in distribution systems. Simplified modeling and formulation of a fault distance calculation from a substation for ground faults in circuits is made using only the discrete voltage and current samples obtained at the substation. The formula in principle seeks to find the value of a line inductance to the fault from the substation by analyzing the transient waveform of phase voltage and current. In particular, in the equivalent circuit of the faulted system, the method applies voltage injection and superposition principle, obtains net fault voltage and current, and calculates the line inductance to the fault as fault distance. The steps for implementing the formula from substation sampled data are detailed and illustrated, followed by validation test results with eleven actual transient faults.**

***Index Terms*—Fault location, self-clearing faults, sub-cycle faults, transitory faults, distribution system.**

I. Introduction

AMONG the seven smart grid characteristics, self-healing tops the list which is, in essence, the grid's immune system [1]. Self-healing is defined as enabling the problematic elements of a system to be isolated and restored to normal operation with little or no human intervention so that the system will result in minimal or no interruption of service to consumers [2]. A self-healing grid will perform continuous, online self-assessments to predict potential problems, detect existing or emerging problems, and initiate immediate corrective responses. Advanced sensors will detect patterns that are precursors to faults, providing the ability to mitigate conditions before the faults actually occur.

As a precursor to self-healing in distribution systems, a distribution fault anticipator project was conducted from late 1990s to mid-2000s, resulting in the confirmation of the proof-of-concept that advanced monitoring and precursor waveform analysis may lead to early warning of apparatus failures and conductor damages [3]. In spite of many promising case studies, there is one fundamental problem with the current status of distribution fault anticipation: no location capability for such failing apparatus or conductors. Incipient faults, both in overhead line and underground cables, show their signature behaviors with fewer than 2 transient cycles before the grid returns to normal behavior. This self-clearing transient fault has its root cause in water accumulation in a cable splice, for example, which leads to an insulation breakdown followed by arc, which in turn causes rapid water evaporation and temporary insulation recovery. In overhead lines, animal contact with the conductor produces similar self-clearing transients, causing damage to the conductor.

The correct location of self-clearing transitory fault is crucially important in prevention of permanent faults and unscheduled outages, and would eliminate costly and time consuming fault locating methods that stress system components exposed to fault currents. The self-clearing fault location, if added to the existing distribution fault anticipation, will give utilities a complete picture of not only what is failing, but where that failure is going to occur [4]. The location of a self-clearing incipient fault would allow electric utilities to quickly and accurately indicate momentary faults, find their location, shorten response time, and improve reliability and reduce operating and maintenance expenses. However, unlike a permanent fault, presently, the location of this type of transient fault has no solution.

Permanent fault location algorithms have traditionally relied on phasor information of voltage and current in calculating line impedance or reactance as the main variable as fault distance [5]–[7]. The phasor is defined and obtained from steady-state sinusoidal signal of voltage and current. Therefore, the fault location algorithms wait for the DC offset to decay and look for the start of the steady-state period of fault signals. Then, using the steady-state sinusoidal signals of, for example, two or more cycles, they calculate the magnitudes and phase angles of the signals to produce phasor information of the signals for the fault distance calculation. Self-clearing transitory faults which last less than 2 cycles, therefore, cannot be located by the conventional fault location algorithms.

Some unconventional approaches have been introduced to detect and locate short lived faults. A transient impedance method was applied, but without verification, to eventually calculate the distance to a fault utilizing the transient waveform generated by the fault of arcing phenomenon [8]. Another approach applied time domain reflectometry and travelling wave incorporating high-speed data recording and triggering with wireless local and remote communication systems [9]. The fault point is determined by identifying the first major point of difference in the TDR pulses, but its accuracy is influenced by the TDR injections on phases for a given fault type. As a practical approach, with numerous circuit breaker trip operations at one customer location, a power company devised a detection scheme of transient faults, with a relay that responded fast

Manuscript received August 01, 2012; revised October 18, 2012; accepted November 27, 2012. Date of current version May 18, 2013. Paper no. TSG-00476-2012.

C. Kim is with the Department of Electrical and Computer Engineering, Howard University, Washington, DC 20059 USA (e-mail: ckim@howard.edu).

T. Bialek and J. Awiylika are with San Diego Gas & Electric, San Diego, CA 92123 USA (e-mail: tbialek@semprautilities.com; jawiylika@semprautilities.com).

Color versions of one or more of the figures in this paper are available online at http://ieeexplore.ieee.org.

Digital Object Identifier 10.1109/TSG.2012.2231442

enough to half cycle voltage and current conditions but did not to the faults that were not initiated near a voltage peak [10]. However, this method was not intended to and could not locate the self-clearing faults.

In addition to the above mentioned approaches and their problems, there are much more difficult problems and challenges in self-clearing fault in distribution systems. Unlike transmission lines, distribution lines are complex and complicated with combined overhead line and underground cable sections, single or double phase laterals and branches, and different conductor sizes and characteristics. Therefore, any attempt to accurately model a self-clearing fault in distribution systems would meet many unknown variables, uncertain parameters, and have to compensate all different conditions which are unknown. Hence, most proposed distribution fault location approaches turn to, for modeling and testing, the principle and routines of the simulation software they rely upon for load flow analysis. It is not surprising therefore that their reported location accuracy is always good.

The objective of this paper is to present an initial investigation of locating self-clearing faults in distribution systems. Our focus is to model the self-clearing faults as simple as possible so that the algorithm can be applied to complex circuits of centrally monitored substations. The principle theory of the self-clearing transitory fault location algorithm combines the conventional injection method at the faulted location, which is to be determined, and the calculation of line inductance as the distance to the location using the voltage and current signals measured at the substation. The theory's main distinctive feature is that it does not need the inductances of the faulted, otherwise, healthy phases or source, the essential information required by most of the (permanent) fault location algorithms. Another important feature of the self-clearing transitory fault location method is that the source inductance of substation is obtained in the process of fault location calculation.

In formulating the principal theory, Section 2 first discusses the rationale of the proposed self-clearing fault location method before fault location formula derivation including limitations and probable errors involved in the formula. The implementation of the derived formula for fault location calculation is illustrated in Section 3. In the last two sections, the test of the self-clearing transitory fault location formula using substation measured data is discussed, followed by the conclusion of the paper and future works.

II. Single Line-to-Ground Fault Location Formulation

A. Assumption and Limitation

The principal approach of this initial investigation is to make a simple model which can be formulated by using only centrally available data at a substation and can apply to a variety of circuits of overhead and underground cable combination radiating from the substation. This approach leads to the elimination of all resistive and shunt components of the circuit. This assumption is acceptably true by the actual measurement results of fault voltage and current. One distinctive approach of the proposed model uses, instead of the overall fault quantities, the net fault voltage and current, which can be obtained by subtracting the nominal voltage and current from the fault voltage and current, respectively, over the time frame of the transitory fault presence. Another distinctive feature of the proposed model is to represent the self-clearing fault condition by injecting the negative voltage at the fault inception time and, employing the superposition principle. The injection of voltage, instead of current, can eliminate the errors that happen for a circuit fault with the centralized monitoring of all circuits at the substation caused by the difference between the pre-fault current level at the monitoring point at the substation and the current of the faulted circuit during the fault. With the superposition principle, only the injected fault inception voltage is considered as the sole source in the fault path, ignoring the main source, then a formula is drawn to calculate the inductance of the line in the path as the distance to the fault using the net fault voltage and current.

In the derivation of fault location formula, the distribution system and the substations of San Diego Gas & Electric (SDG&E) are used and from which fault data were obtained for testing of the developed algorithm. In particular, the substation transformer(s) are Y-connected and directly grounded from the neutral point, and a 3-phase capacitor bank is connected to the substation bus. The centralized substation measurements are on the bus therefore the measured voltage is the bus voltage and the measured current is the current from the main source which includes the combined current from multiple circuits connected to the bus.

The simplified modeling and formulation brings limitation (and error) inevitably. The fault resistance is completely ignored even though there must be some resistance in the fault path, which causes error in calculation. The developed model is primarily for short distribution lines and ignores the shunt capacitance which is assumed to be small compared with the substation capacitor bank. Despite all these limitations and probable errors involved, the attempted formulation is still meaningful in that it is a new approach conceived to try to find the location of self-clearing faults with hope that it can be properly adjusted in the field trials and thus be improved further for specific distribution systems. The details of which are illustrated in the sections to follow.

B. Formulation for Self-Clearing Fault Location

Let's start our discussion with a circuit diagram shown in Fig. 1 for a single line-to-ground fault on phase A at the location x in the assumed substation and one circuit configuration. The circuit is equivalently expressed with a sinusoidal source E_s with source inductance L_s, parallel capacitance C, inductance of the circuit from the substation to the location of the fault, L_{line}, and the inductance of the circuit from the fault location to the end of the circuit, L_r, with all resistive components ignored. The only variables measurable at the substation, through CTs and PTs, are the current flowing through the source impedanceL_s and the bus voltage across the capacitor C. The approach intends to calculate the inductance L_{line} to x by using only the substation measured voltages and currents.

Now, assuming that at time $\mathrm{t} = 0$ (or $\mathrm{t} = \mathrm{tF}$) a self-clearing phase A ground fault occurs with zero fault resistance, then at that instant, the voltage at x becomes zero. The voltage zero incident can be represented as an injection of a negative voltage,

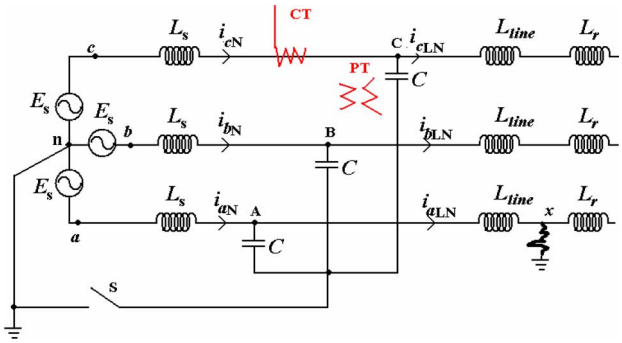

Fig. 1. Circuit Diagram for a Single Line-to-Ground Fault on Phase A.

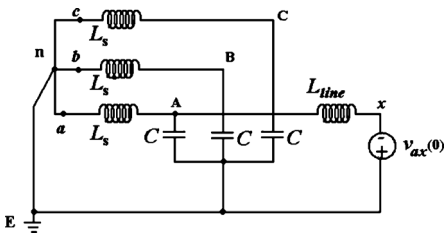

Fig. 2. Reduced Circuit Diagram of a Phase A Single Line-to-Ground Fault by the Application of Voltage Injection and Superposition.

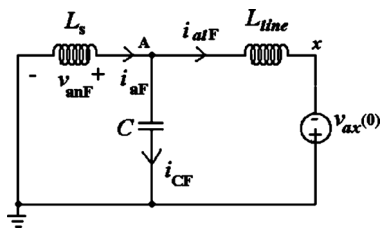

Fig. 3. Further Reduced Circuit Diagram of Fig. 2.

$-\mathrm{V_{ax}}(0)$, into the location x of the system for the very short period. The accurate estimation of the injected voltage at x requires exact information of the fault location, which is yet to be determined; therefore, we estimate it to be the value of voltage at the measurement point at the fault inception time, $\mathrm{V_{aN}(tF)}$. By the superposition principle, since the focus is only in the change of voltage and current, termed "net fault voltage and net fault current" due to the self-clearing fault, not in the total value by the injected voltage and the source voltage, the source voltage E_s is removed from the equivalent circuit while keeping $-\mathrm{V_{ax}}(0)$ or $-\mathrm{V_{ax}(tF)}$, between x and the ground. The negative voltage injection and superposition principle now reduces the circuit diagram of Fig. 1 to the circuit of Fig. 2.

By rearranging the circuit of Fig. 2, the two branches of phases B and C can be eliminated because they are shorted to the neutral and ground, and thus only phase A components of source inductance and capacitance remain, along with the line inductance to the fault, as illustrated in Fig. 3.

The currents of $\mathrm{i_{aF}}$, $\mathrm{i_{CF}}$, and $\mathrm{i_{alF}}$ and the voltage $\mathrm{v_{anF}}$ are the net fault currents and voltage, respectively, contributed only by the injected voltage source. The net current $\mathrm{i_{aF}}$ and the net voltage $\mathrm{v_{anF}}$ can be obtained by subtracting the measured normal, pre-fault, values from the measured values at fault. Now, the problem is equivalent to the transient response of a DC voltage switched on to the circuit at $\mathrm{t} = 0$ (or $\mathrm{t} = \mathrm{tF}$).

From Fig. 3, we can draw the following equations:

$$i_{aF} = i_{alF} + i_{CF}, \tag{1}$$

$$v_{anF}(t) = -L_s \cdot \frac{di_{aF}(t)}{dt}, \tag{2}$$

and

$$v_{anF}(t) = L_{line} \cdot \frac{di_{alf}(t)}{dt} - V_{aN}(tF), \tag{3}$$

where $di_{aF}(t)/dt$, $di_{alF}(t)/dt$ are the first time derivatives of the net fault phase current and the net line current, respectively.

Then, combining (1) and (2) leads to the following net fault voltage equation:

$$V_{anF}(t) = -L_s \cdot \frac{di_{aF}(t)}{dt} = -L_s \cdot \left[\frac{di_{alF}(t)}{dt} + \frac{di_{CF}(t)}{dt}\right]. \tag{4}$$

Equation (4) can be further reduced to the following equation:

$$V_{anF}(t) = -L_s \cdot \frac{di_{alF}(t)}{dt} - L_s \cdot C \cdot \frac{d^2 v_{aF}(t)}{dt^2}, \tag{5}$$

where $d^2 v_{aF}(t)/dt^2$ is the second derivative of the net fault voltage.

By rearranging (3) with respect to the net line fault current, and substituting it with the net line fault current in (6) lead to the final fault distance inductance equation for phase to ground fault with terms of the net voltage and current:

$$L_{line} = \frac{-v_{anF}(t) + V_{aN}(tF)}{\frac{di_{aF}(t)}{dt} - C \cdot \frac{d^2 v_{aF}(t)}{dt^2}}. \tag{6}$$

The term $v_{aN}(tF)$ is the value of voltage at the measurement point at the onset of the breakdown. A breakdown, at the early stage of insulation deterioration, occurs at the maximum voltage point, positive or negative [10]; however, as the deterioration further develops, it may occur at a lower voltage level.

In case of the absence of the capacitor bank, by simply eliminating the term with C in (6), the following fault distance equation can be drawn:

$$L_{line_{NC}} = \frac{-v_{anF}(t) + V_{aN}(tF)}{\frac{di_{aF}(t)}{dt}}. \tag{7}$$

C. Compensation of Mutual Coupling

When seeking the formulation of the fault location, we focused only on measurable data instead of estimated and assumed ones including the cable impedance and capacitance and even the cable length. Therefore the coupling component is not included in the formulation, which, undoubtedly, brings errors in distance estimation. However, there is a rough compensation scheme available for this simplified method following the sequence component analysis for unbalanced earth fault wherein the ratio of residual voltage and the phase voltage is calculated as $3\mathrm{K}/\{2+\mathrm{K}\}$ and the ratio of the residual current and the phase current as $3/\{2+\mathrm{K}\}$, where K is the sequence impedance ratio

of zero- and positive-sequence of the line, Z0/Z1 [11]. Therefore, combining the above two ratios together, it is interpreted that the phase impedance is K times smaller than the residual impedance. Following this ratio of K, and from the successful results of applying sequence component method in transient analysis [12], [13], the proposed method may approximately compensate for coupling effect the calculated distance L_{line} in (6) and (7) by dividing it by the sequence impedance ratio K, and thus producing "compensated distance", L_{line}/K.

III. Implementation of the Formula

The implementation of the derived formula for digital numerical calculation of the variables from the sampled voltage and current signals, requires the following four parameters to be acquired or processed from the acquired data: (i) net phase fault voltage and current, (ii) the voltage at fault inception, and (iii) the first discrete derivatives of the net phase fault current and the net residual fault current, and (iv) the second discrete derivative of the net fault voltage.

This section describes the steps to be taken to derive the four parameters from measured data and the process of applying the formula for the distance to fault at each sample point. However, the data measurement system and its background are first explained.

A. Power Quality Monitoring System

To meet the keen interests of utilities' in fault location, EPRI launched a multi-year base research program to (a) evaluate different approaches of fault location and (b) install them within power quality monitoring systems. The project helped to implement the latest permanent fault location approaches within the PQView data management and analysis system, integrated with other distribution and outage management system components such as electrical database, GIS, and operational databases [14]. PQView is the premier industry tool for managing large databases of power system quality monitoring information. It is used by many utilities around the world as the foundation for collecting from a variety of different monitor types, managing the database of disturbance and steady state data, reporting on performance, and providing alarms and notifications for problem conditions [15].

At SDG&E, beginning in 1993, eight power quality monitors were installed, and by 2005 a total of 40 power quality monitors integrated with PQView, called PQNodes, were installed. Creelman substation is one substation where a PQnode was installed at each of the two buses: North and South buses. The North bus was supplied by a 69/12 kV 25 MVA transformer and served 3 circuits (970, 971, and 973), and the South bus served 6 circuits (235, 236, 237, 972, 974, and 975) supplied by two transformers: 69/12 kV 20 MVA and 15 MVA. The PQnodes installed at the Creelman Substation from which the data for testing the sub-cycle fault location formula were obtained were Dranetz-BMI PQNode 8010 [16] which captured triggered and periodic steady-state waveforms with simultaneous sampling rate of 128 points per 60 Hz cycle for all three phase voltages, three phase currents, and the residual current. Each PQnode was set to record, when triggered, 2 cycles of pre-triggered event waveforms and 12 cycles of post-triggered event. The trigger was set to respond to the voltage or current magnitude change of $\pm 10\%$ or more.

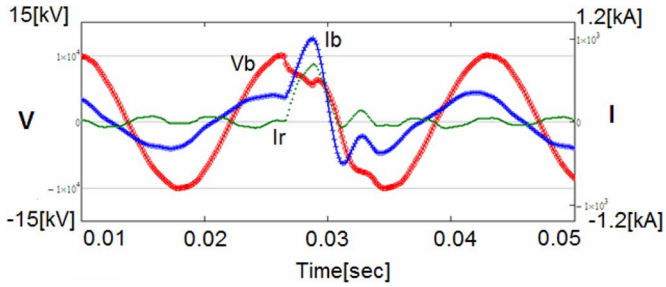

Fig. 4. A portion of PQNode captured waveforms of a sub-cycle fault.

B. Raw Voltage and Current Data

The first step of the process is to read the captured raw data of a PQNode which contains at least 1 cycle of normal and several cycles of post-trigger (transient fault) waveforms of voltages and currents. Fig. 4 is one example of such waveforms which shows the phase voltage (Vb) and current (Ib) as well as the residual current (Ir) of a phase B single line-to-ground sub-cycle fault which lasts about 1/2 cycle period. This particular waveform was captured at 01:49 AM on August 21, 2006, and in about 8 hours later, at 09:35 AM, a cable fault occurred at 5.02 miles from the substation.

C. Net Voltage and Current Derivation

Separated by the fault inception time stamp, say tF, the captured PQNode data of voltage and current are to be split into two, synchronized data components: pre-fault data and post-fault data of a full cycle length or more. Synchronization of both data sets is very important because the former is to be subtracted from the latter for the net fault value. The synchronization is established in the following manner. First, the normal data over the entire captured data length can be obtained by taking a single cycle of pre-fault samples, starting from the first sample point to the 128th sample which covers one complete normal cycle, and then by concatenating the same single cycle after the full cycle pre-fault samples repeatedly until the combined sample number is the same as that of the captured raw data. Second, the entire captured raw samples, including the 1 cycle pre-fault normal sample in the beginning, are used as the fault data. Then, the net fault data are obtained by subtracting the normal data from the fault data, sample by sample. The graph in Fig. 5 depicts the net fault voltage (VbF) and the net fault current (IbF) of the phase B fault waveform shown in Fig. 4. The normal voltage of phase B is also displayed for reference.

D. Differentiation of Net Fault Current and Net Fault Voltage

The fault distance formula contains the first derivative of the net fault current $(\text{dI}\underline{\text{a}}\text{F}/\text{dt})$ and the second derivative of the net fault voltage $(\text{d}^2\text{VaF}/\text{dt}^2)$ for a Phase A fault, for example. Numerical differentiation of digitized signals is derived from the definition that the first derivative (dy/dt or dy in simplified notation) of a time varying signal (y) is the rate of change of y with time t. Under the constant and identical time interval (Δt) between adjacent sample points, the simplest algorithm

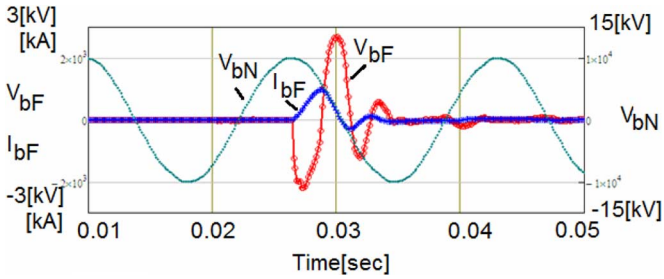

Fig. 5. Net fault voltage and net fault current of the raw data of Fig. 5. The voltage of phase B, VbN, is also displayed for reference.

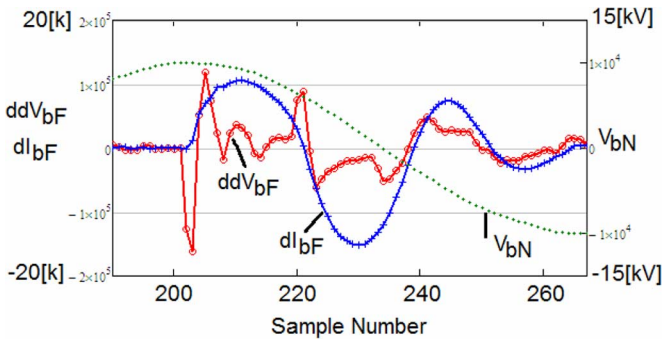

Fig. 6. The first derivative net fault current (dIbF) and the second derivative of the net fault voltage (ddVbF) referenced with the normal voltage (VbN).

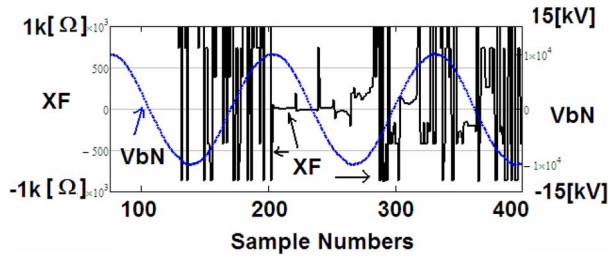

Fig. 7. Example of fault distance (XF) calculation referenced with the normal phase B voltage (VbN).

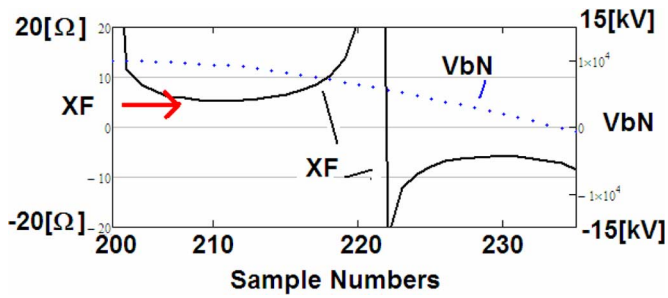

Fig. 8. Details of the fault distance (XF) for the 1/4 cycle period after fault inception, referenced with the normal phase B voltage (VbN).

for computing a first derivative at sample time n, termed as the first order forward difference formula for first derivative, is expressed by: $\mathrm{dIaF}^1(\mathrm{n}) = [\mathrm{IaF}(\mathrm{n}+1) - \mathrm{IaF}(\mathrm{n})]/\Delta\mathrm{t}$. By applying Taylor expansion, a second order centered difference formula for the first derivative is obtained by: $\mathrm{dIaF}^2(\mathrm{n}) = [\mathrm{IaF}(\mathrm{n}+1) - \mathrm{IaF}(\mathrm{n}-1)]/[2\Delta\mathrm{t}]$. For the data tested, the second order first differentiation was the best choice with reduced sensitivity to the random, white noise components contained in the raw data.

For the second derivative for net fault voltage, even though there are many ways to obtain the second derivative, applying the above first derivative twice is found to be effective. Fig. 6 illustrates the first derivatives of the net fault current (dIbF) and the second derivative of the net fault voltage (ddVbF) of Fig. 5. The normal phase B voltage is displayed as well for reference purpose. Due to the discrete time step calculation for the derivatives, the x-axis now changed to sample numbers from the time in second. As indicated above, the 128 sample length corresponds to 1 second long data.

E. Fault Location Calculation

With the necessary parameters produced in the above steps, the formula for locating self-clearing transitory fault is executed. Note that in the normal situation, the net fault voltage and net current or its derivative are close to zero, therefore the output of the formula would produce a result of infinity or indeterminate distance to fault. To avoid this "divide-by-zero" error, if the net fault value is near zero, a small number is added to the denominator of the formula to produce the distance with a big number, positively or negatively, so that the result would be ignored and referred as no-fault situation.

Note also that the calculation is on the digitized data and, therefore, the output is produced at each sampling point. Due to the use of the first and second derivatives, the output could be very sensitive to noise in the waveform. However, the tests reveal that there is a certain period in which the values of the formula are maintained with consistency, however short the period may be. In the experimentation, about quarter cycle or half cycle would be enough to produce stabilized trajectory for determining the inductance value associated with the fault.

Fig. 7 illustrates the sample by sample result of the fault distance reactance (XF), which is converted with 60 Hz power frequency from the inductance distance (L_{line}) of the faulted phase B, with spiky regions of normal period and consistent and stabilized values after the fault inception at near the sample number 200. The stabilized period lasts about 1/2 cycle referenced with the normal voltage.

Fig. 8 shows the expanded view of Fig. 7 around sample points of 200–235, about 1/4 cycle length, referenced again with the normal voltage. The determination of the fault distance reactance is determined in the quarter cycle period after the inception of fault since a normal voltage level at the inception is applied to the faulted circuit (injection) and the shorter time window represents more accurate transient response of the sub-cycle self-clearing fault voltage. As pointed by an arrow in the figure, the fault distance reactance obtained is 5.3 [ohms].

While it would be easier for testing and validating the developed formula with the simulated data from model of self-clearing faults in distribution systems, there is no available self-clearing model or simulation. Therefore, it seems that the only way possible to test the derived formula is with actual data. This has the advantage of validation against actual data and serves as a real performance benchmark.

TABLE I
SELF-CLEARING FAULTS AND CALCULATED FAULT DISTANCES

Rec #	Bus/Ckt	Cause	DF[mile]	XF [Ohm]
175398	S 970	Cable Fault	2.76	1.35
178645	S 970	LBE	4.29	2.60
173212	S 971	Cable Fault	4.05	3.55
175554	S 971	Cable Fault	5.07	3.99
174278	S 973	Cable Fault	1.93	2.45
174068	S 973	Cable Rack	4.08	2.75
175697	S 973	Cable Fault	5.02	2.93
176522	S 973	Cable Fault	5.02	3.55
177794	N 975	Cable Rack	2.58	2.34
177797	N 975	Cable Rack	2.58	2.25
175957	N 975	Cable Fault	2.82	2.68

IV. TESTING WITH SUBSTATION MEASURED DATA

This section reports the preliminary validation of the developed approach using the PQNode measured data. To collect testing data for the developed self-clearing transitory fault location formula, SDG&E's outage listing for years 2006 and 2007 is utilized. In connection with the power quality monitoring, SDG&E produces yearly outage reports per circuit of all substations, isolating and or damaged devices, occurrence time stamps, and fault distances in miles. From the list, only subcycle transient faults at the Creelman substation are selected. Next, the data which closely matched the outages are downloaded from the PQnode via PQView data management system. The data obtained from PQView, 11 ground faults involving underground cables and accessories, were always slightly (or more) ahead in time of the outage in the listing, clearly revealing that the self-clearing transient faults, at their initiation at least, were not captured by clearing devices but, once self-cleared, gradually developed to permanent faults which were then successfully cleared.

A. Self-Clearing Fault Data

The 11 self-clearing faults are listed in Table I. The first column is SDG&E's outage record number, and the second column shows a bus-circuit pair indicating a bus (South or North) of the 12 kV Creelman substation the faulty circuit is connected to. The third column lists the cause of the failure associated with the outage, and the acronym LBE in the cause column stands for "load break elbow" which is a connection point that can be disconnected while energized and carrying load in underground systems. The fourth column indicates the fault distance (DF) in miles from the substation to the fault or fault clearing device as reported in the outage listing. The last column provides the fault distance in reactance (XF) calculated by the formula developed in this paper.

An exact and direct validation cannot be made because of the two reasons: (i) the outage report shows the fault distance only with miles, which in non-homogenous network would have a non-linear relationship with the line impedance, and (ii) the fault distance in the report indicates the distance from the substation to either a fault clearing device or a fault damaged device, the locations of which are usually not the same. Therefore, it is expected that discrepancy in the locations, at least for some of the faults, between the outage report and the algorithm calculation is inevitable.

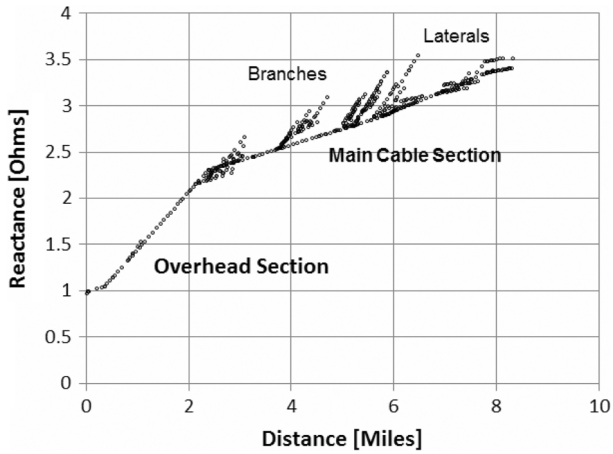

Fig. 9. The plot of the cumulative $\{\text{reactance, distance}\}$ pairs of circuit 970.

Another component of expected discrepancy is that the distribution circuits are not homogeneous; instead, they are combined by overhead line sections with underground cable sections and by single or double phase cable laterals and branches. Therefore, the result of the validation of the developed formula must be interpreted in the proper perspective. The result reported here with actual network is very different from the ones produced by a method using simulated data, both developed from the same principle.

In all, there are multiple error-causing sources in the circuit and fault location indication. However, despite these error causing sources, the test of the formula with real data still has its merits as it may give a general sense of the formula and its acceptability for utility engineers and provide a good experimental experience for betterment of the derived formula.

B. Validation of the Formula

As stated above, the direct comparison between the true fault distances in miles and the calculated distance in reactance for the circuits with mix of overhead lines and underground cables is difficult. Therefore, we decided to perform qualitative validation of the developed formula in the following fashion. First, we acquire the circuit section data and retrieve a pair of quantities, cumulative positive sequence reactance and cumulative distance from the substation of all devices, equipment and facilities in the circuits. The scatter plot of the cumulative $\{\text{reactance, distance}\}$ pairs of the circuit 970 is illustrated in Fig. 9.

As mentioned above, the circuit is not homogeneous and nonlinear and with 3-phase overhead and cable sections and 1-phase and 2-phase branches and laterals. Second, for the qualitative validation, for each of the circuits listed in Table I, we mark a pair of the result, for each of the self-clearing faults, made from the calculated fault distance XF and the fault distance DF reported in the outage list. If the $\{\text{XF, DF}\}$ pair sits on the cumulative reactance-distance scatter plot of a circuit, then we can say that the calculation accurately locates the self-clearing fault. The $\{\text{XF, DF}\}$ pair farther away from the reactance-distance pair points is poorer in accuracy.

The validation results by circuits follow accompanied by Figs. 10–13. In the figures, the small filled dots are, as in Fig. 9,

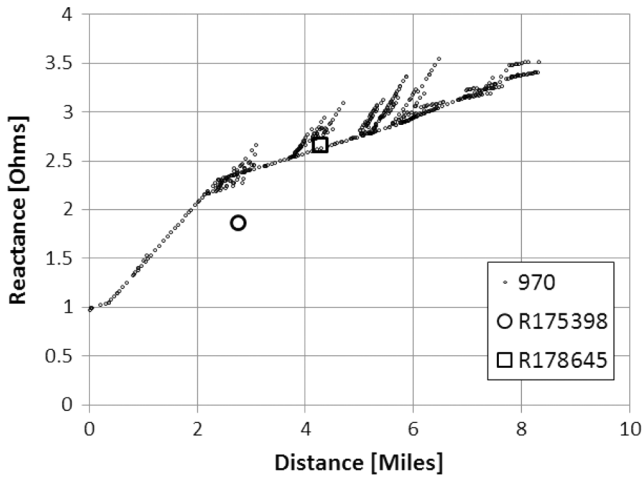

Fig. 10. Test results of the faults on Circuit 970.

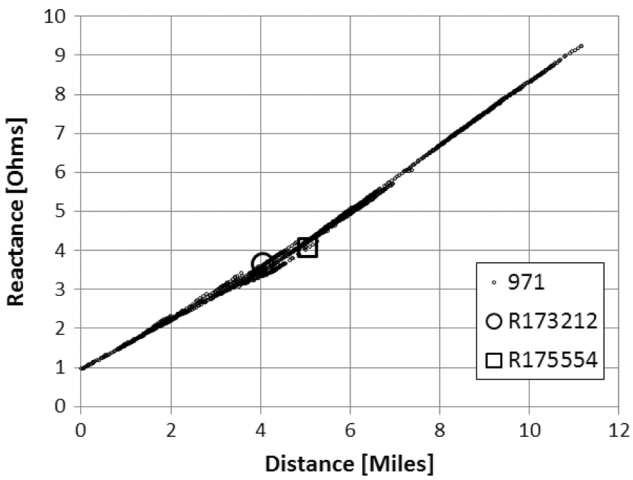

Fig. 11. Test results of the faults on Circuit 971.

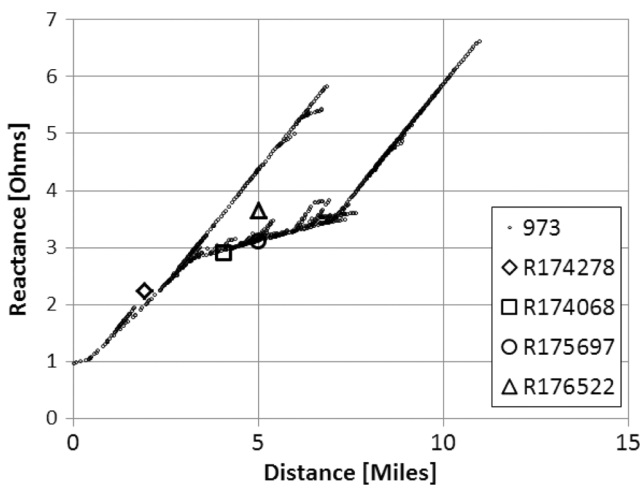

Fig. 12. Test results of the faults on Circuit 973.

the (reactance, distance) pair of the circuits. On the other hand, unfilled big symbols of diamond, circle, square, or triangle are the {XF, DF} pairs for given faults, of which the record number of each is, starting with letter R, written next to the symbol in the legend box.

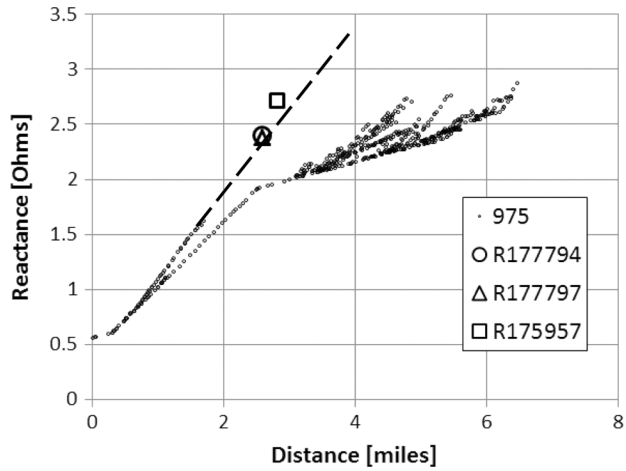

Fig. 13. Test results of the faults on Circuit 975.

Test Result for Circuit 970: In Fig. 10, the two self-clearing faults are placed on the circuit 970 reactance-distance scatter points. The LBE failure at 4.26 miles is pin-pointed while the cable fault at 2.76 miles, which is at the border line between overhead and cable sections, is far off and poorly pointed.

Test Result for Circuit 971: Fig. 11 depicts the two faults caused by cable failure on and close to the reactance-distance scatter points of the circuit. The circuit is nearly linear and looks homogeneous even though the change in the conductor characteristics at 4 miles is unmistakable.

Test Result for Circuit 973: Fig. 12 shows the 4 marks for the faults on the Circuit 973. The circuit is complicated with linear and non-linear sections with overhead branches and cable laterals. None of the (XF, DF) pairs sits right on the scatter points of the circuit; however, none is far off from the points either.

Test Result for Circuit 975: As depicted in Fig. 13, all three (XF, DF) pairs of the faults on Circuit 975 sits on the extended line of the second overhead line section of the circuit. They are far off the correct section of the underground cable. This circuit has more cable laterals and branches than other circuits. It seems as if the formula "sees" the circuit's second overhead line section as the apparent impedance of the entire circuit.

C. Discussions

As illustrated for Circuit 971, the simple formula works satisfactorily for the circuit of combined sections overhead and underground cable as far as the circuit in general has a linear conductor characteristic, a single slope made by the conductor reactance over the unit distance, namely x/d. On the other hand, when a circuit has multiple conductor characteristics or the x/d slopes, the results are mixed with acceptable and poor accuracies.

Even taking into consideration the ambiguity in the "fault distance" indicated in the outage list and subsequently by the fact the clearing devices are always closer to the substation than the damaged devices or actual faults, there definitely are a few large discrepancies in results, one of which is the R175398 fault on

Circuit 970. Therefore, a further investigation should be conducted for practical applications of the developed formula. First and foremost, the detailed and accurate fault distance should be acquired from the outages. Second, more data and more validation tests are required to build confidence and certainty in the results produced by the developed formula. Third, a further investigation of including ignored variables to the developed model and estimating them should also be considered.

V. Conclusion

This paper discussed a simplified formula for locating self-clearing transitory faults by employing voltage injection at the faulted location and the superposition principle to calculate the line reactance to the fault using only the voltage and current signals measured at substation. A distinctive feature of the fault distance formula was that it did not need the inductances of the line or sources. Another feature of the proposed formula is that it uses the net fault quantities instead of the overall fault quantities. The detailed steps and processes of the formula implementation for practical application were detailed along with test results with 11 actual transitory faults involved in underground cable and cable racks. The validation of the formula was performed in a qualitative manner since for the outage list the relationship between the "fault distance" in miles were not clear as well as consistent enough to indicate if it was meant for the actual faults or the clearing devices. The validation highlighted two things: (i) the simplified model worked for the complicated distribution networks comprised of overhead and underground sections, especially so with better accuracy when the circuit sections are in conductor characteristics of impedance per distance relatively linear, and (ii) there were also the examples where the results of the formula had poor accuracy. The problems led us to expand our investigation into the following three subjects: (i) establishment in process and procedure to record the location of faults not clearing devices; (ii) continuation of the self-clearing fault data collection and validation tests, and revision of the formula, to build confidence in utilizing the method; and (iii) investigation of a way to include more variables to the developed model. We are currently working on how we improve and apply and coordinate the developed formula with our distribution/outage management system.

References

[1] "The Smart Grid: Introduction," Litos Strategic Communication, East Providence, RI, Report, 2008.

[2] "A systems view of the modern grid: Appendix A1–Self-heals," National Energy Technology Laboratory (NETL), Mar. 2007.

[3] B. Don Russell and C. L. Benner, "Intelligent systems for improved reliability and failure diagnosis in distribution systems," *IEEE Trans. Smart Grid*, vol. 1, no. 1, Jun. 2010.

[4] J. M. Fangue, "Distribution fault anticipator," presented at the Southwest Electric Distribution Exchange, Corpus Christi, TX, May 2, 2006.

[5] E. Schweitzer, "A review of impedance-based fault locating experience," in *Proc. 15th Annual Western Protective Relay Conf.*, Spokane, WA, Oct. 24–27, 1988.

[6] D. Novosel, D. Hart, E. Udren, and J. Garitty, "Unsynchronized two-terminal fault location estimation," *IEEE Trans. Power Delivery*, vol. 11, no. 1, pp. 130–138, Jan. 1996.

[7] T. Takagi, Y. Yamakoshi, M. Yamaura, R. Kondow, and T. Matsushima, "Development of a new type fault locator using the one-terminal voltage and current data," *IEEE Trans. Power Apparatus Syst.*, vol. PAS-101, pp. 2892–2898, 1982.

[8] S. Horton and N. van Luijk, "Low voltage fault detection and localization using the Topas 1000 disturbance recorder," *Electric Power Quality and Utilization Mag.*, vol. 2, no. 1, pp. 27–32, 2006.

[9] J. Livie, P. Gale, and A. Wang, "Experience with on-line low voltage cable fault location techniques in Scottish power," in *19th Int. Conf. Electricity Distribution (CIRED)*, Vienna, Austria, May 21–24, 2007.

[10] L. Kojovic and C. Williams, "Sub-cycle detection of incipient cable splice faults to prevent cable damage," in *Proc. IEEE Power Engineering Society Summer Meeting*, Seattle, WA, Jul. 2000, vol. 2, pp. 1175–1180.

[11] *Network Protection and Automation Guide*. Paris, France: Alstom, 2002.

[12] P. Perracci, M. Meunier, and L. Berthet, "An equivalent circuit for earth-fault transient analysis in resonant-grounded distribution power networks," in *Proc. Int. Conf. Power Systems Transients (IPST)*, Sep. 1995, pp. 359–364.

[13] W. Huang and R. Karczmarek, "Symmetrical components for transient regime applications in MV systems," in *Proc. Int. Conf. Power Systems Transients (IPST)*, Lyon, France, June 2007, Paper No. 118.

[14] M. McGranaghan, T. Short, and D. Sabin, "Using PQ monitoring infrastructure for automatic fault location," in *19th Int. Conf. Electricity Distribution (CIRED)*, Vienna, Austria, May 2007.

[15] "PQView—The industry standard power quality database management and analysis software," Electrotek Concepts, 2011 [Online]. Available: www.pqview.com/pqview/

[16] "8101 PQnode user's guide, dranetz-BMI," 1998.

Charles Kim (M'90–SM'06) received the Ph.D. degree in electrical engineering from Texas A&M University, College Station, TX, in 1989 in the subject area of power system automation and high impedance fault in distribution systems.

Currently, he is an Associate Professor in the Department of Electrical and Computer Engineering at Howard University, Washington, DC. His research interests include failure detection, anticipation, and prevention in safety critical systems. Since 2007, he has collaborated with SDG&E in sub-cycle incipient fault location in the distribution systems.

Thomas Bialek (M'82) received the B.Sc.(EE) and M.Sc.(EE) degrees from the University of Manitoba, Canada, in 1982 and 1986, respectively. He received the Ph.D. degree in electrical engineering from Mississippi State University in 2005.

He is currently with San Diego Gas & Electric Company as a Chief Engineer on the Smart Grid Team. His present responsibilities involve smart grid strategy and policy issues.

Jude Awiylika received the B.Sc.(EE) degree from Howard University, Washington, DC, in 2002.

He is currently with San Diego Gas and Electric in the Transmission Engineering department. His present responsibilities involve engineering projects to Harden Transmission Lines against wildfires and high winds and upgrade existing line capacity to carry and deliver more power.